Economic Geology
Vol. 98, 2003, pp. 1213–1224

Source of Iron for Sulfidation and Gold Deposition, Twin Creeks Carlin-Type Deposit, Nevada

John Fortuna,* Stephen E. Kesler,† and David P. Stenger**

Department of Geological Sciences, University of Michigan, Ann Arbor, Michigan 48109

Abstract

This study was undertaken to determine the source of iron in Comus Formation sedimentary rocks that were sulfidized during deposition of gold in the Megapit area of the Twin Creeks Carlin-type deposit. Sedimentary rocks in and near the Megapit contain ferroan dolomite, largely as overgrowths on iron-poor dolomite. Iron to form these overgrowths appears to have been released from mafic volcanic rocks that are interlayered with the sedimentary rocks. These igneous rocks have undergone two stages of hydrothermal alteration. The first stage involved formation of albite and iron-rich chlorite, possibly caused by interaction with seawater. The second stage involved destruction of the iron-rich chlorite by illite or sericite, which released iron to form ferroan dolomite in the sedimentary rocks. Comparisons show that transfer of iron from the igneous rocks to the sedimentary rocks can account for the present distributions of iron in these rocks. Relative to basalts, Comus Formation igneous rocks are enriched in iron and potassium. These results suggest that ferroan dolomite in sedimentary rocks is not solely a product of diagenetic processes and can form when iron is released from adjacent iron-bearing igneous rocks. Recognition of this additional mechanism for formation of ferroan dolomite expands the range of geologic settings that can be favorable for formation of gold deposits formed by sulfidation.

Introduction

Sulfidation has been implicated in ore deposition in a number of Carlin-type gold deposits, although very little information has been gathered on the mineralogical site and origin of the iron that underwent sulfidation (Hofstra et al., 1991; Kuehn and Rose, 1992, 1995; Hofstra, 1994; Stenger et al., 1998; Hofstra and Cline, 2000; Cail and Cline, 2001). Two possible sources of iron were evaluated for the Twin Creeks deposit, where sulfidation associated with gold deposition had been documented previously (Stenger et al., 1998).

During sulfidation, iron in host rocks reacts with sulfur in an invading hydrothermal solution, causing deposition of pyrite. Loss of reduced sulfur from solution to form pyrite destabilizes dissolved gold bisulfide complexes, leading to deposition of gold. In most Carlin-type deposits, sedimentary rocks are the dominant or only host rocks for ore and are therefore the most likely source of iron for sulfidation. At Twin Creeks, however, iron could have been derived from sedimentary or interlayered igneous rocks of the ore-hosting Comus Formation, and this might reflect depositional, diagenetic, or possibly later alteration processes that affected these rocks. Selection between these possibilities is important to genetic models for Carlin-type and other gold deposits that form by sulfidation, as well as to selection of rock units most likely to host undiscovered deposits.

Geology, Mineralogy, and Age of Twin Creeks Mineralization

The Twin Creeks mine is located on the eastern flank of the Osgood Mountains, approximately 75 km northeast of Winnemucca, Nevada (Fig. 1). It is just east of a north-northeast-striking linear zone of Carlin-type gold deposits, including Pinson, Preble, and Getchell, that is known as the Getchell trend (Cline, 1999; Cail and Cline, 2001). Twin Creeks is currently owned and operated by the Newmont Mining Company, and it is the third largest primary gold-producing mine in North America with annual production (1999) of 760,000 oz and reserves of 87 million metric tons (Mt) averaging 0.079 oz/short ton (st) (Thoreson et al., 2000). At the time of this study (1997- 1998), ore was mined from the Vista open pit in the northern part of the deposit (Chimney Creek), as well as from the Megapit in the southern part of the deposit (Rabbit Creek), which was the focus of this study.

Gold in the Megapit area at Twin Creeks is hosted by the Ordovician-age Comus Formation (Ordovician sequence of Stenger et al., 1998), which consists of fine-grained siliciclastic and silty carbonate sediments interbedded with basalt tuffs and flows, and mafic to ultramafic sills (Bloomstein et al., 1991; Thoreson et al., 2000). These rocks are overlain by the Antler-age (Late Devonian-Early Mississippian) Roberts Mountains thrust sheet (Leviathan thrust sheet of Osterberg, 1990; Osterberg and Guilbert, 1991; Stenger et al., 1998), which consists largely of basalt, tuffaceous sediments, and chert of the Ordovician Valmy Formation in the Twin Creeks area (Crafford, 2000; Thoreson et al., 2000). The Pennsylvanian-Permian Etchart limestone, which was deposited on these rocks, is overlain by the Sonoma-age (Late Permian) Golconda thrust sheet that is made up in this area of interbedded limestone, chert, siltstone, sandstone, and minor basalt flows of the Mississippian-Permian Havallah sequence (Ferguson et al., 1952; Silberling and Roberts, 1962; Thoreson et al., 2000). Paleozoic rocks west of Twin Creeks have been intruded by the Cretaceous-age Osgood granodiorite stock, dikes, and sills (Hotz and Wilden, 1964; Silberman et al., 1974). Related intrusive rocks are found in and below the Chimney Creek section of the Twin Creeks deposit (Osterberg, 1990; Osterberg and Guilbert, 1991; Hall et al., 2000; Thoreson et al., 2000). Tertiary-age tuffs and volcaniclastic

*Present address: R&M Environmental and Infrastructure Engineering, Inc., 7901 Oakport Street, Suite 4700, Oakland, California 94621-2015.

**Present address: Lehman Brothers Equity Research, Metals and Mining Group, 745 7th Avenue, New York, New York 1001.

†Corresponding author: e-mail, skesler@umich.edu

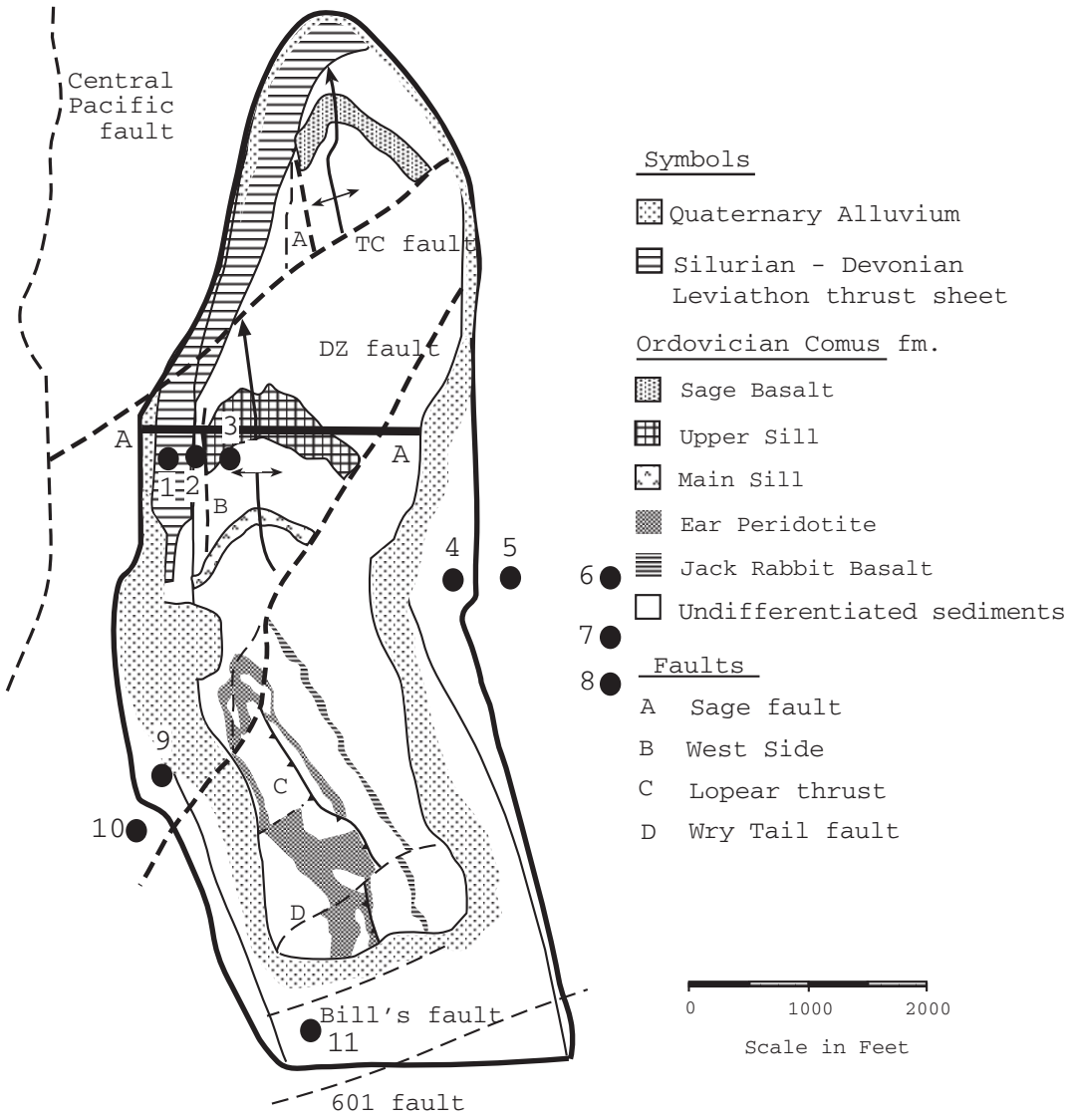

FIG. 1. Schematic geologic map of the Megapit area of the Twin Creeks Carlin-type deposit, showing location of cross section (A-A'), which is shown in Figure 5, as well other drill holes from which samples were obtained. 1 = R-346, 2 = R-338, 3 = R-209, 4 = R-352, 5 = R-510, 6 = R-492, 7 = R-230, 8 = R-70, 9 = R-476, 10 = R-546, 11 = CTW-278 and 12 = CTW-150. Inset shows location of Twin Creeks.

sedimentary rocks crop out north and east of the mine area, and alluvial cover that thickens from northwest to southeast covers the Megapit area and reaches depths of 200 m at its southern end (Bloomstein et al., 1991; Thoreson et al., 2000). Deformation of the Comus Formation during emplacement of the Roberts Mountains thrust formed the Conelea anticline, an east-verging overturned fold that extends the entire length of the Megapit and is cut by the northeast-striking right-lateral Twin Creeks and DZ faults (Fig. 1; Stenger et al., 1998; Thoreson et al., 2000).

Mineralizing fluids at Twin Creeks appear to have migrated up the nose of the Conelea anticline and spread laterally into favorable sedimentary layers (Stenger et al., 1998; Simon et al., 1999). Igneous rocks in the Comus Formation are largely barren or weakly mineralized, although they are pervasively altered to fine-grained muscovite (sericite) and illite in many areas. Mineralization took place in seven stages including an initial stage of diagenetic pyrite. Gold is found almost exclusively in arsenian pyrite that was deposited during stages III, V, and VI of this sequence (Simon et al., 1999). In contrast to most Carlin-type deposits in which alteration consists largely of kaolinite and illite (Hofstra and Cline, 2000), gold in the northern part of the Megapit is also associated with adularia (Simon et al., 1999). This adularia appears to have formed when mineralizing solutions remobilized potassium in the Comus Formation igneous rocks, which are unusually potassium rich (see below). Adularia from stages III and IV mineralization, as well as prestage III, vein-hosted illite in the northern part of the Megapit, yields $^{40}Ar/^{39}Ar$ ages of about 42 Ma and represents the age of much of the gold mineralization

in the Megapit area (Groff et al., 1997; Hall et al., 2000). Illite that pervasively replaces volcanic rocks in areas of high-grade gold ore yields Cretaceous $^{40}Ar/^{39}Ar$ ages of 105 to 103 Ma that represent a major alteration event and possible deposition of some gold (Hall et al., 2000).

Geochemistry of Iron in Sedimentary Rocks

Sedimentary rocks from the Comus Formation in the Twin Creeks ore zone include fine-grained limestones, fine-grained, laminated calcareous shales and siltstones, and fine to coarse-grained calcareous volcanic tuffs (Fig. 2). Information on the bulk composition of these sedimentary rocks was obtained from analyses of a suite of 492 hand samples of limestone and laminated shale obtained from drill core in the Megapit ore zone (Stenger et al., 1998). A ternary plot of CaO, MgO, and Fe_2O_3 concentrations in these samples contains three clusters (Fig. 3A). Samples with high gold grades fall largely along the trend between clusters B and C, particularly at its high-iron end, whereas samples in cluster A have low gold values (Fig. 3B).

In Figure 3A, cluster A near the CaO apex consists of relatively pure limestones; cluster B in the lower center consists of carbonate-bearing shales. Average loss on ignition (LOI) values, which consist largely of CO_2 in these rocks, reach nearly 40 percent for the limestones (cluster A) and about 20 percent for the carbonate-bearing shales (cluster B). Average silica and alumina contents of the two clusters differ significantly, with the carbonate- bearing shales averaging about 50 percent SiO_2 and 7 percent Al_2O_3 and the limestones containing only a few percent of each oxide. The higher MgO and Fe_2O_3 contents of the carbonate-bearing shales in cluster B reflect the presence of significant siliciclastic debris of volcanic origin. Cluster B falls on a mixing line between the compositions of dolomite, which makes up the matrix of these rocks, and Comus Formation igneous rocks, which make up the clastic fraction (Fig. 3C). Stenger et al. (1998) showed that the carbonate matrix in these rocks consists of dolomite with ferroan dolomite rims containing an average of 8.6 percent Fe.

The trend extending toward cluster C and the Fe_2O_3 apex in Figure 3A includes compositions of altered carbonate-bearing shales. Decarbonatization of the carbonate-bearing shales could produce iron enrichment no greater than that of the average composition of Comus Formation igneous rocks (Fig. 3C). It would not account for rocks with compositions in cluster C which average 76 wt percent SiO_2, only 2 wt percent CaO + MgO, and 8 wt percent LOI that is made up largely of OH in hydrous silicate minerals rather than CO_2. These rocks probably formed by cation leaching and silicification, leaving only clay minerals with or without illite or sericite, pyrite, and quartz. Decarbonatization, silicification, and cation leaching of this type are commonly associated with gold in Carlin-type deposits (Hofstra and Cline, 2000).

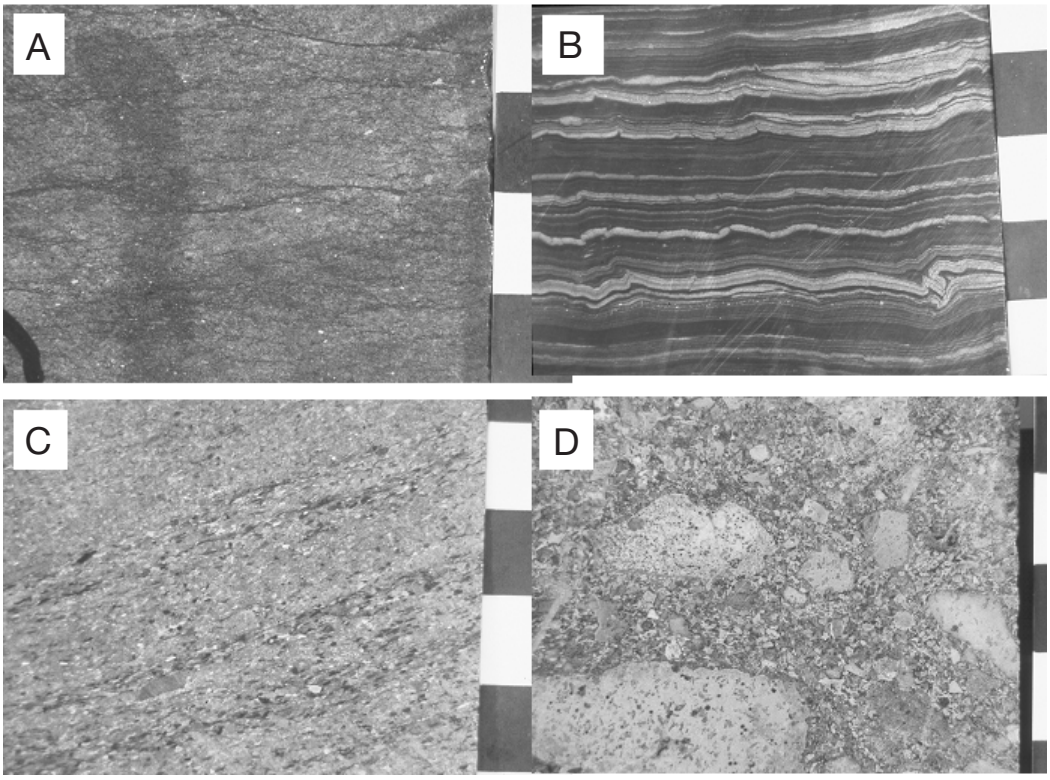

FIG. 2. Sedimentary and fragmental volcanic rocks in the Ordovician sequence at Twin Creeks (scale is divided into 1-cm units in all photographs). A. SED-174-99: fine-grained limestone. B. TWE-17-1854: laminated calcareous shale. C. TWE-17-1821: medium-grained, calcareous shale. D. TWE-17-1580: coarse-grained basaltic tuff.

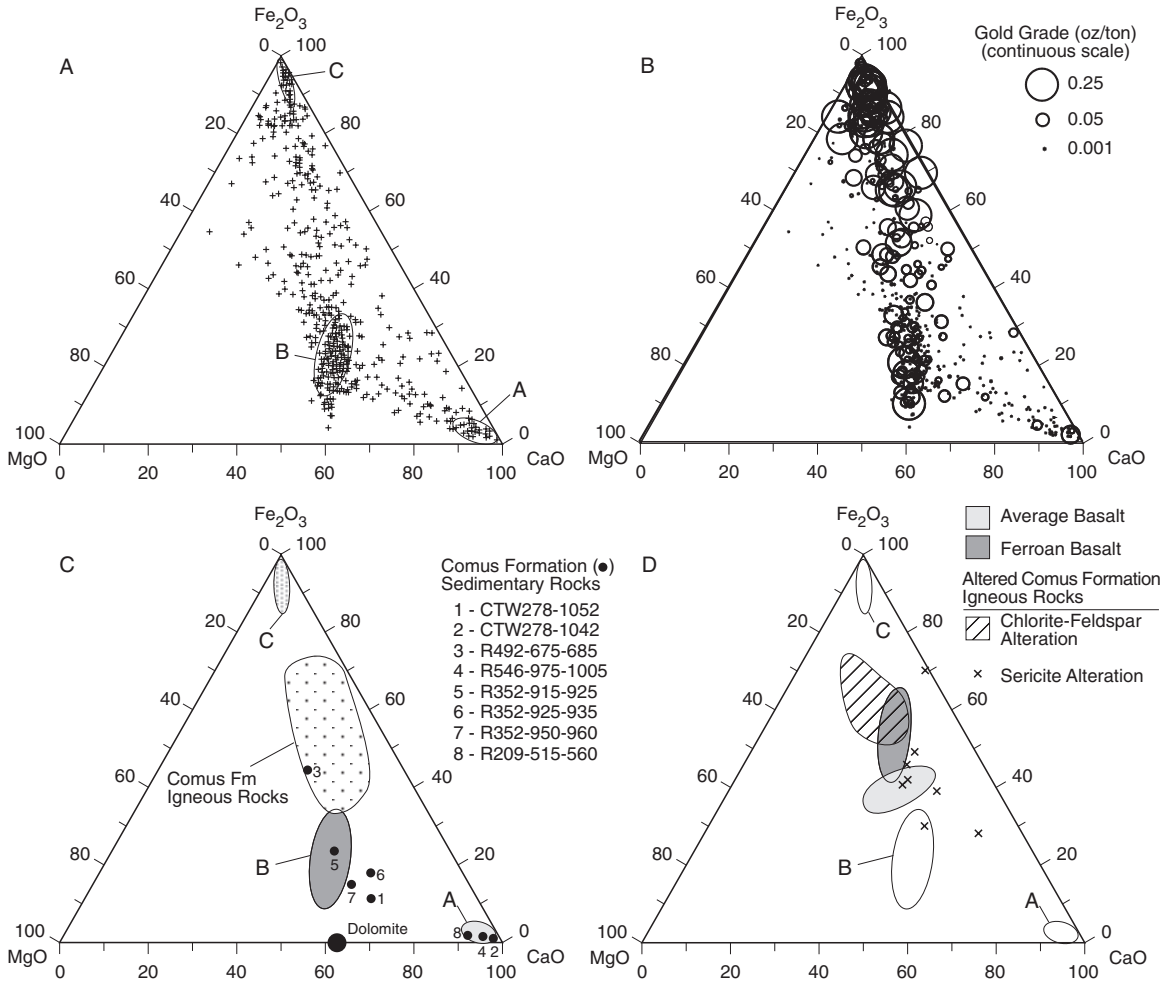

FIG. 3. Ternary plots of CaO, MgO and Fe_2O_3 concentrations (wt %) in sedimentary and igneous rocks. A. whole-rock chemical analyses of 492 sedimentary rocks in the Megapit ore zone at Twin Creeks. Clusters represent relatively pure limestone (A), carbonate-bearing shales containing ferroan dolomite (B) and decarbonated shales (C). B. The same plot as A with gold grades of samples shown as circles (note that most gold-rich samples fall along the trend between clusters B and C. C. Whole-rock compositions of Comus Formation igneous rocks and sedimentary rocks (Table 1) compared to clusters A, B, and C from the Comus Formation, D) whole-rock compositions of igneous rocks, including average basalt, ferrobasalt, and altered Comus Formation igneous rocks compared to clusters A, B, and C from the Comus Formation Chlorite and sericite alteration are shown separately (data from Irvine and Baragar, 1971; Gill, 1981; McBirney, 1983; Pefit and Fornari, 1983).

Samples of barren sedimentary units located immediately outside the ore zone but correlating with mineralized layers in the ore zone were studied petrographically to provide additional information on the composition of sedimentary rocks that underwent mineralization (Table 1). Compositions of most of these samples fall in or near clusters A and B in Figure 3C. Samples CTW-278 1042, R-546 995-1005, and R-209 515-560 are typical limestones with high CaO contents and LOI values of 31 to 37 wt percent. CO_2 analyses for these samples (Table 1) confirm that their LOI values are almost entirely due to CO_2. Samples CTW-278 1052, R-352 915-925, R- 352 925-935, and R-352 950-960 are carbonate-bearing shales with significantly higher SiO_2 contents and lower but still significant LOI and CO_2 contents. Iron in these rocks is hosted largely by pyrite and ferroan dolomite. The pyrite forms framboids and isolated euhedral grains that are very different from ore-stage arsenian pyrite; the pyrite is preore (diagenetic) in origin. Assuming that all sulfur in these rocks is hosted by pyrite (Table 1), between 1 and 32 percent of the iron in these samples has been sulfidized (i.e., is in pyrite). The remainder is largely in ferroan dolomite, which forms fine-grained subhedral to anhedral grains, as well as overgrowths on earlier carbonate grains, especially in the carbonate-bearing shales (Fig. 4A). Electron microprobe analyses of ferroan dolomites in the carbonate-bearing shale samples range from 2.3 to 5.4 wt percent Fe_2O_3 (Table 2), somewhat lower than the iron contents of ferroan dolomites in the ore zone. R-492 675-685, which plots between clusters B and C in Figure 3, is the only sample in this group with a high sulfur content. This sample also has a low LOI, is enriched in iron relative to the other samples, and has a higher potassium content reflecting a higher illite abundance, consistent with decarbonatization, illitization, and silicification.

TABLE 1. Chemical Analyses of Core Samples of Barren Sedimentary Rocks of the Comus Formation from outside the Megapit Ore Zone at Twin Creeks

Drill hole	CTW-278	CTW-278	R-492	R-546	R-352	R-352	R-352	R-209
Depth (ft)	1,052	1,042	675-685	995-1,005	915-925	925-935	950-960	515-560
	1	2	3	4	5	6	7	8
SiO_2	59.38	22.55	63.67	12.33	65.93	66.89	55.15	14.94
Al_2O_3	8.44	4.06	12.23	1.00	5.68	4.47	2.86	1.69
Fe_2O_3	1.51	0.50	4.43	0.71	3.32	2.75	3.26	1.00
MnO	0.02	0.02	0.04	0.02	0.08	0.08	0.12	0.03
MgO	3.71	0.81	2.24	1.95	3.67	3.18	6.05	3.55
CaO	9.72	38.82	3.3	45.75	7	9.08	12.83	40.99
Na_2O	0.04	0.02	0.09	0.04	0.05	0.05	0.04	0.03
K_2O	2.47	1.15	4.12	0.22	2.02	1.53	0.93	0.47
TiO_2	0.39	0.19	0.99	0.03	0.39	0.25	0.13	0.07
P_2O_5	0.17	0.05	0.24	0.12	0.19	0.13	0.71	0.04
LOI	12.74	31.42	8.23	37.53	11.37	11.84	16.82	36.54
Total	98.60	99.58	99.58	99.69	99.70	100.26	98.89	99.35
CO_2	11.0	30.7	3.5	37.2	10.2	11.1	16.4	35.7
S	0.387	0.065	1.29	0.115	0.037	0.151	0.453	0.119

Major elements were analyzed by fusion-ICP with detection limit of 0.01%; CO_2 and S determined by Leco analysis with detection limit of 0.01% for CO_2 and 0.003% for S

TABLE 2. Electron Microprobe Analyses of Diagenetic (Ferroan) Dolomites from Sedimentary Rocks of the Comus Formation outside the Megapit Ore Zone at Twin Creeks

Grain	7	10	13	14	15	2-1	2-11	2-12
MgO	20.49	18.85	18.41	18.22	18.42	21.63	17.40	16.29
CaO	31.46	30.31	30.46	31.01	30.94	28.83	32.31	31.75
MnO	0.02	0.06	0.00	0.03	0.07	0.10	0.16	0.16
FeO	2.07	2.36	2.59	2.31	2.46	2.25	3.78	5.01
CO_2[1]	48.33	45.85	46.48	45.67	45.94	47.68	46.77	45.87
Total	102.37	97.43	97.94	97.24	97.82	100.49	100.42	99.07
Normalized to 2 cations								
Mg	0.926	0.898	0.882	0.871	0.876	0.991	0.813	0.760
Ca	1.022	1.037	1.049	1.066	1.057	0.949	1.084	1.065
Mn	0.000	0.001	0.000	0.001	0.002	0.003	0.004	0.004
Fe	0.052	0.063	0.069	0.062	0.076	0.058	0.099	0.131

[1]CO_2 calculated by stoichiometry

Geochemistry of Iron in Igneous Rocks

Samples of Comus Formation igneous rocks outside the ore zone were obtained from a thick basalt unit in drill hole TC-5, approximately 3,000 m from the Megapit. During field work in 1998, this basalt unit was correlated with the Main sill, a prominent unit in the ore zone (Stenger et al., 1998; Thoreson et al., 2000). Main sill basalt from hole TC-5 consisted originally of an ophitic intergrowth of a mafic mineral, plagioclase, and large grains of iron-titanium oxide (Fig. 4B). All of these minerals have been altered extensively; the mafic mineral consists now of abundant Fe-rich chlorite and lesser amounts of ferroan dolomite, and the plagioclase consists largely of albite and/or K feldspar, with local illite or sericite. The original magmatic iron-titanium oxide has been altered to an intergrowth of rutile and Fe-rich chlorite (Fig. 4C), which appears to reflect an original late-magmatic exsolution texture (Haggerty, 1976; Lindsley, 1976). Trace amounts of magmatic apatite are unaltered. Iron in the TC-5 Main sill basalt is largely in chlorite, which contains 29 to 33 wt percent FeO, enough to classify it as daphnite (Table 3). The presence of Ca, Na, and K and a large excess of octahedrally coordinated Al (Al^{VI}) relative to tetrahedrally coordinated Al (Al^{IV}) in some analyses are consistent with mixed chlorite-corrensite compositions (Shau et al., 1990). Daphnite makes up 20 to 35 percent of most samples and accounts for 6 to 10.5 wt percent Fe in the whole- rock analysis. It is therefore the main source of iron in the rock. Fe-Ti oxide in these rocks has a very low Fe/Fe + Ti ratio, consistent with the high Fe/Fe + Mg in the coexisting chlorite (Rumble, 1976).

Main sill samples from TC-5 were compared to Main sill samples in the ore zone from several drill holes along section A-A' that crosses gold ore in the central part of the Megapit (Figs. 1 and 5). The Main sill does not host significant gold in this section, but is directly adjacent to ore. Correlation of the Main sill in the two areas is supported by their unusually large

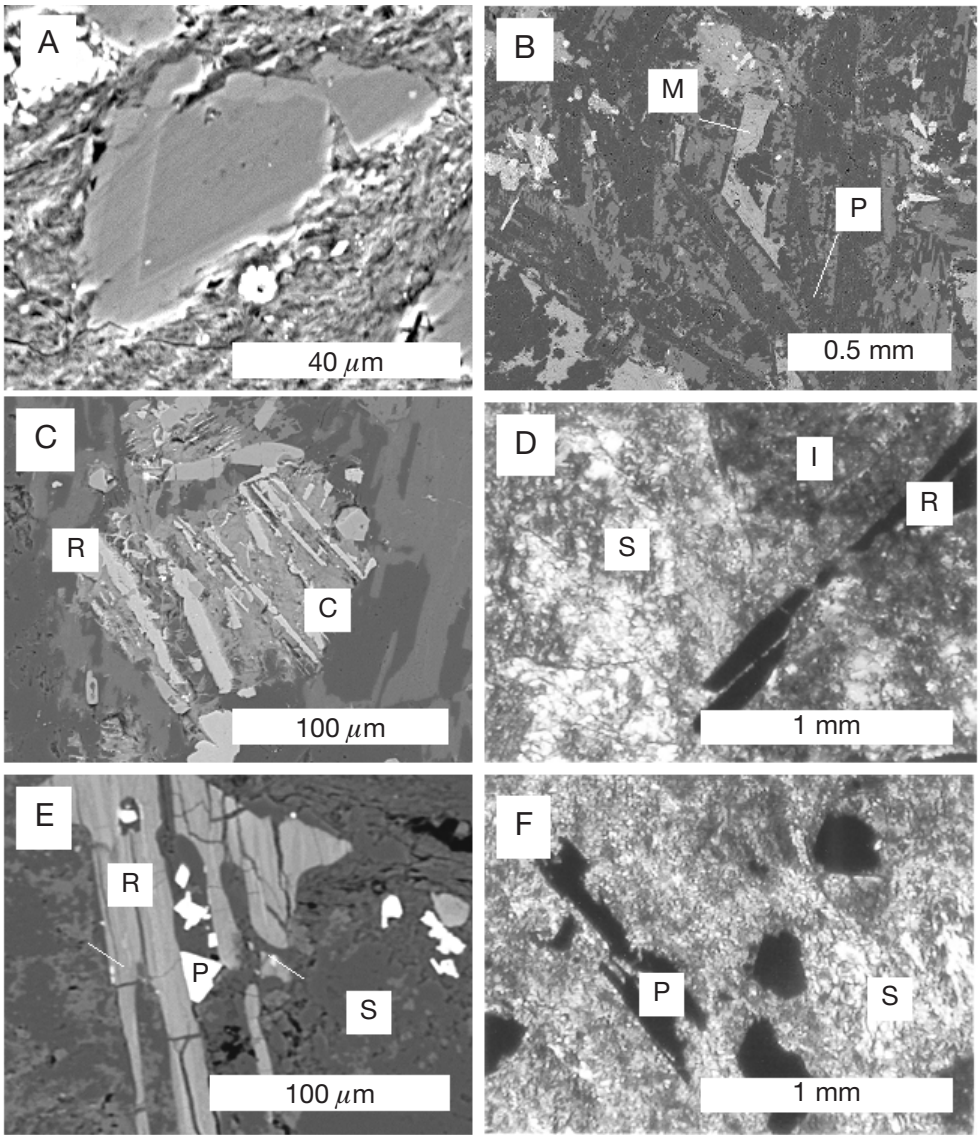

FIG. 4. Secondary electron–back-scattered electron (SEM-BSE) images and photomicrographs of thin sections from: A) iron-rich rim (light) around iron-poor diagenetic dolomite from SED-174 989, B) Feldspar-chlorite altered Main sill in TC 5 1803 showing ophitic intergrowth of mafic mineral (M) altered to Fe-rich chlorite, and plagioclase (P) altered to albite and minor illite. C) Detail from TC 5 1803 showing intergrowth of rutile (light gray) and Fe-rich chlorite (dark gray). D) Photomicrograph (plane light) of sericite-altered Main sill from mine area (R81-652) showing rutile (dark) laths cutting across illite (I) that replaces the groundmass and sericite (S) replacing phenocryst. E) SEM-BSE image of sericite-altered Main sill from mine area (CTW 402 899) showing rutile laths (R) in matrix of sericite (S) with small amount of pyrite (P). F) Photomicrograph (plane light) of sericite-altered Main sill from mine area (CTW 402 849) showing rutile (R) laths replaced by pyrite (P) in matrix of sericite (S).

remnant Fe-Ti oxide phenocrysts. Additional samples from igneous units above the Main sill were obtained from drill hole CTW-150 in the northern part of the Megapit (Fig. 1). All of these rocks showed evidence for two stages of alteration. The first stage of alteration is similar to that described above for TC-5 basalts and included replacement of mafic minerals by iron-rich chlorite. The original Fe-Ti oxide mineral has been altered to rutile and iron-rich chlorite; feldspars have been altered to albite and locally abundant K feldspar. This alteration generally preserved original rock textures, although it replaced most magmatic minerals. The second stage of alteration involved replacement of this assemblage by widespread sericite or illite and local adularia (Fig. 4D). In most samples, rutile is not altered (Fig. 4D), although some samples contain rutile associated with small amounts of pyrite (Fig. 4E) and a few contain an opaque mineral, probably originally rutile, that has been completely replaced by pyrite (Fig. 4F). The distribution of pyrite in the Main sill does not show any systematic relationship to gold ore.

Nature of Iron Exchange between Igneous and Sedimentary Rocks

The formation of abundant iron-rich chlorite and ferroan dolomite in stage I alteration and its complete removal during

TABLE 3. Electron Microprobe Analyses of Chlorite in the Main Sill outside the Megapit Ore Zone at Twin Creeks

Hole number	TC-5	TC-5	TC-5
Sample depth (ft)	1,755	1,803	2,051
SiO_2	26.49	29.80	27.03
TiO_2		0.12	0.05
Al_2O_3	21.87	15.35	18.23
FeO	32.90	29.16	29.28
MnO	0.01	0.01	0.19
MgO	6.37	13.19	12.49
CaO		0.08	0.12
Na_2O	0.01	0.01	0.01
K_2O	0.03	0.01	0.00
F		0.33	0.32
Total	87.68	88.06	87.72
Cations			
Si	2.88	3.18	2.92
Ti		0.01	0.00
Al	2.80	1.93	2.32
Fe	2.99	2.60	2.64
Mn	0.00	0.00	0.02
Mg	1.03	2.10	2.01
Ca	0.01	0.01	0.01
Na	0.00	0.00	0.00
K	0.00	0.00	
F		0.11	0.11
Total	9.72	9.95	10.03
n	6	7	10

Results shown are representative of chlorite compositions for each sample; cation normalization did not detect any Fe_2O_3; therefore, all iron is reported as FeO; formula are reported as a unit half-cell based on 14 14 anhydrous oxygen; *n* = number of analyses for each sample

stage II alteration suggests that iron was liberated from the igneous rocks during the second stage of alteration. This possibility can be evaluated by comparing compositions of the Main sill basalt outside the ore zone (TC-5) to those of Main sill basalt in the ore zone. Al_2O_3 and TiO_2 in these rocks are not strongly correlated, suggesting that one or both were mobile during alteration and thus limiting the use of the isocon approach that has been used for such comparisons in other Carlin-type deposits (Hofstra, 1994; Hofstra and Cline, 2000; Cail and Cline, 2001). Although variations in the compositions of the samples must be compared in multicomponent space to assure that all variables are recognized, most of the important changes can be shown in Fe_2O_3-CaO-MgO plots. Figure 3D shows that three samples of TC-5 Main sill basalt and two samples of Main sill from the mine area, all with similar first-stage, chlorite-feldspar alteration, form a well-defined cluster. All but one of the Main sill samples that have undergone extensive second-stage, illite-sericite alteration plot below the cluster of chlorite-feldspar altered samples, suggesting that they have lost iron relative to calcium and magnesium.

If iron was released from the igneous rocks, it could have been added to the interbedded sedimentary rocks. This possibility can be evaluated by comparisons based on data from the Twin Creeks bench composite database. This database contains analytical information for 20-ft (true thickness) bench composites of drill core from ore and adjacent barren zones. All samples have associated X, Y, and elevation data and were analyzed for gold, total carbonate, acid-insoluble carbon, total iron, arsenic, antimony, mercury, and sulfide and sulfate sulfur (Stenger et al., 1998). Each sample was also assigned a lithology code according to the dominant rock type present in that 20-ft interval. For the purposes of this study, these samples were separated into groups consisting entirely of sedimentary or igneous rocks, as indicated by the drill logs. Samples that consisted of mixtures of these two rock types or that included other rock types were eliminated. Histograms of the abundance of gold in these two lithologic groups (Fig.

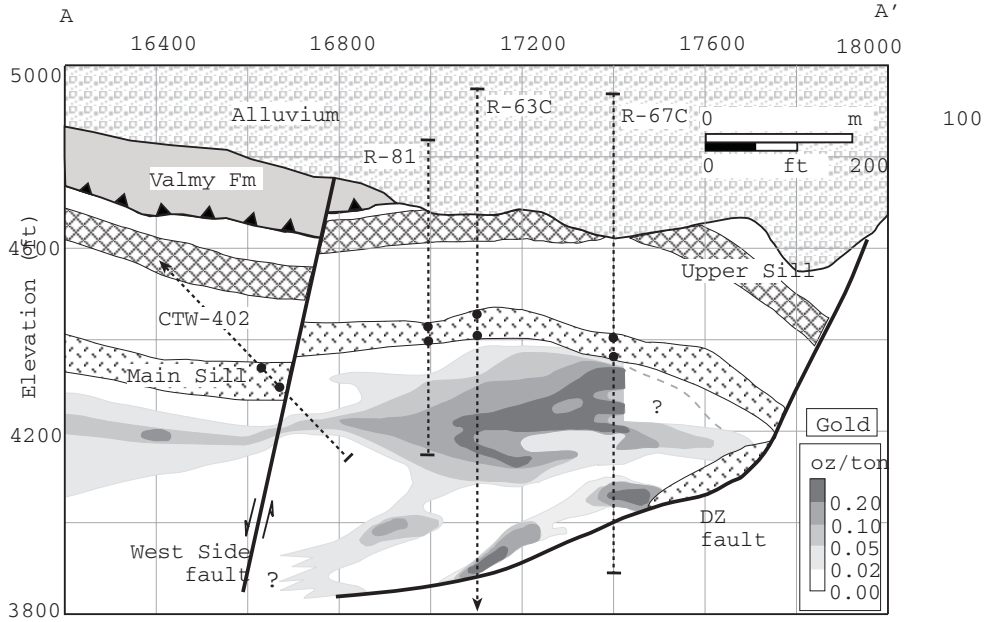

FIG. 5. Geologic relations along cross section A-A' in Figure 1, showing distribution of gold ore and location of analyzed samples from drill holes in the Main sill (Table 4).

TABLE 4. Chemical Analyses of Igneous Rocks from the Main Sill in the Megapit Ore Zone at Twin Creeks (R-63, R-67, R-81, 402) and from a Thick Basalt Unit Thought to Correlate with the Main Sill outside the Ore Zone (TC)

Drill hole	R-63	R-63	R-67	R-67	R-81	R-81	402	402	TC-5	TC-5	TC-5
Depth (ft)	510	560	564	584	598	652	849	899	1755	1803	2051
SiO_2	40.61	48.76	44.41	54.41	48.41	38.06	46.21	49.00	49.89	54.38	51.87
Al_2O_3	12.44	21.15	18.78	24.19	16.46	17.32	14.78	19.10	16.46	16.12	16.31
Fe_2O_3	10.86	6.90	6.79	1.50	11.96	6.28	8.80	6.38	11.79	7.91	8.54
MnO	0.13	0.05	0.10	0.03	0.06	0.08	0.10	0.07	0.09	0.09	0.12
MgO	4.01	0.13	3.11	1.16	3.88	2.49	2.71	2.43	2.26	2.98	3.50
CaO	12.06	2.73	6.13	2.50	3.83	13.78	6.49	5.02	5.15	2.91	3.26
Na_2O	0.61	1.24	0.57	2.01	2.05	2.71	0.35	1.07	3.49	4.36	5.61
K_2O	1.05	3.12	4.37	3.46	1.59	1.45	3.66	3.31	1.74	3.53	2.60
TiO_2	2.61	2.01	1.65	2.64	2.97	1.35	2.48	1.80	1.54	1.59	1.70
Cr_2O_3	<0.01	0.01	<0.01	<0.01	<0.01	<0.01	<0.01	<0.01	0.02	<0.01	<0.01
P_2O_5	0.35	0.26	0.22	0.35	0.55	0.21	0.37	0.25	0.87	0.92	0.92
LOI	14.58	10.08	11.38	7.30	7.24	15.81	13.41	11.11	6.43	4.20	4.68
Total	99.31	97.80	97.51	99.55	99.00	99.54	99.36	99.54	99.73	98.99	99.11
Sulfate S	<0.01	0.01	<0.01	<0.01	<0.01	<0.01	0.02	0.02	0.02	<0.01	0.01
Sulfide S	0.23	4.01	3.00	0.30	0.13	0.08	4.04	2.49	0.04	0.01	0.01
Inorganic C	3.20	1.10	2.45	0.85	1.10	3.25	2.55	1.90	1.20	0.60	0.70

Locations of drill holes shown in Fig. 1; all samples analyzed by Chemex Labs, Inc., Sparks, Nevada; major oxides analyzed by XRF with detection limit of 0.01 wt %; sulfate by acid/H_2O leach, determined gravimetrically with detection limit of 0.01 wt %; sulfide by HNO_3-bromide digestion, determined gravimetrically with detection limit of 0.01 wt %; inorganic carbon determined by LECO method with detection limit of 0.05 wt %

6) confirm that Comus Formation sedimentary rocks contain about one order of magnitude more gold than do igneous rocks (note that values along the x-axis of these plots differ by an order of magnitude).

The iron contents of Comus Formation igneous rocks at Twin Creeks are also considerably higher than those of the sedimentary rocks and they do not form simple normal populations (Fig. 7). The distribution of iron contents in the igneous rocks is skewed to the left and that in the sedimentary rocks is skewed to higher values, suggesting that they may have exchanged iron. This possibility can be tested in a general way by fitting calculated normal populations to the observed distributions. For example, the original distribution of iron in the unaltered igneous rocks has a mean of 8.5 wt percent iron and a variance of 1.2 and is represented by curve A (Fig. 7A). A smaller population of these samples with the same mean and variance shown by curve B can be used to represent samples that have lost iron. If they lost 3 percent iron, curve B would be shifted to the left to form curve C. The distribution of iron that would result from this loss is shown by curve D, which is the sum of populations C and A minus population B. Curve D is a close approximation to the present distribution of iron in the igneous rocks. Similarly, the present distribution of iron in unaltered sedimentary rocks can be shown by curve A (Fig. 7B), which has a mean of 3.65 wt percent Fe and a variance of 1.25. We can select an arbitrary subset of this population with the same mean and variance (curve B) and add 3 percent iron to it to form a new population (curve C) and add this population to population A minus B. The resulting curve, D in Figure 7B, is very similar to the actual distribution of iron in the sediments. Thus, exchange of iron from the igneous rocks to the sedimentary rocks might account for the observed distributions.

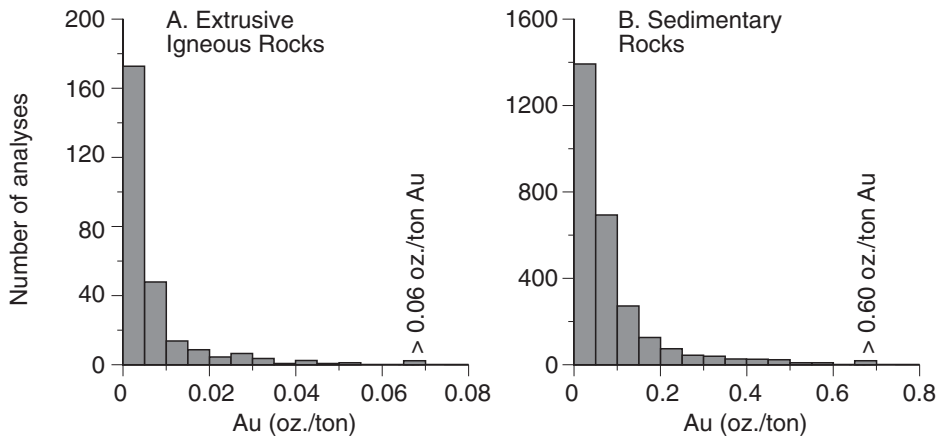

FIG. 6. Histograms showing distribution of gold in extrusive igneous rocks (A) and sedimentary rocks (B). Note difference in gold scales for the two diagrams.

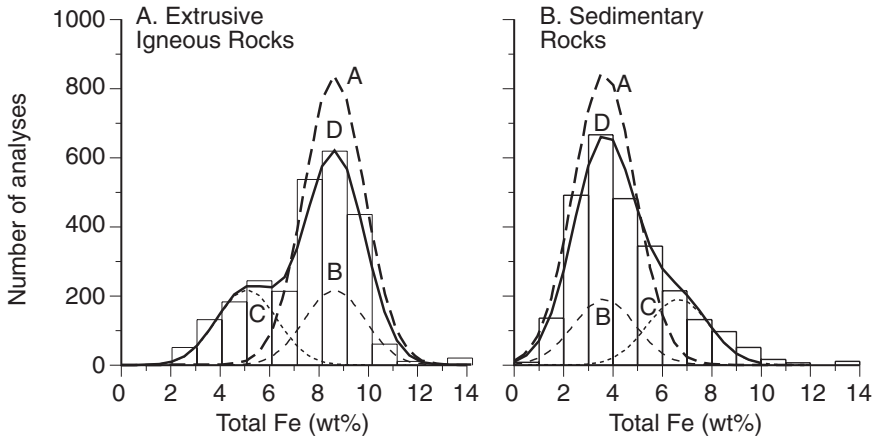

FIG. 7. Histograms showing abundance of iron in extrusive igneous rocks (A) and sedimentary rocks (B). In both diagrams, curve D (solid line) represents present distribution of iron and curve A (long dashed lines) represents hypothetical original distribution of iron. Curves B and C (shorter dashed lines) represent the hypothetical distribution of iron in samples that were affected by removal of iron from the extrusive rocks and addition of iron to the sedimentary rocks, changing the overall distribution of iron in the populations from that of curve A to that of curve D, as explained in the text.

Timing and Geologic Environment of Iron Exchange

Observations summarized above suggest that Comus Formation sedimentary rocks were enriched in iron by a two-stage alteration sequence. First, mafic minerals in the igneous rocks were altered to form iron-rich chlorite and local ferroan dolomite. Then, sericite-illite alteration of the igneous rocks released iron, which migrated into adjacent sedimentary rocks to form ferroan dolomite overgrowths. This ferroan dolomite provided the necessary Fe to precipitate sulfur from mineralizing solutions. As noted above, this sericite has Ar-Ar ages of 105 to 103 Ma and was probably related to hydrothermal circulation around the Osgood stock or its precursors (Hall et al., 2000).

Two aspects of the Comus Formation igneous rocks appear to be especially relevant to this iron exchange process. First, the stage one alteration assemblage in the basalts is similar to that of spilites or basalts that have interacted with seawater during submarine emplacement (Hall, 1990). Seawater-rock interaction is a common part of the diagenetic history of submarine volcanic rocks and almost certainly took place during deposition of the Comus Formation. This interaction did not produce the intense magnesium metasomatism characteristic of discharge zones in seawater hydrothermal systems (Mottl, 1983; Seyfried, 1987). Instead, original magmatic minerals were replaced by low-grade, metamorphic minerals including epidote, albite, and chlorite, which are more widespread in spilite terranes (Mottl, 1983). Although chlorite in most spilitic alteration is magnesium rich, iron-rich chlorites like those in the altered Comus Formation basalts have been reported from spilites at modern midocean ridges and in ancient systems in Taiwan (Alt et al., 1985, 1998; Shau and Peacor, 1992).

The most important factors governing formation of iron-rich chlorite are temperature and sulfur content of the altering fluid (Alt, 1999). Solubility of iron in most sea-floor systems increases dramatically with temperature, suggesting that high-temperature systems would remove iron from the rock (Seyfried, 1987). In addition, the activity of reduced sulfur must be low to avoid formation of pyrite. Bryndzia and Scott (1987) have shown that relatively small changes in f_{S2} or f_{O2} values can result in large variations in chlorite composition, and similar stability relations have been shown for other mafic minerals, including biotite and amphibole (Popp, 1976; Tso et al., 1979). Field studies document decreased Fe/Fe + Mg ratios in a wide variety of mafic minerals, including garnet, staurolite, hornblende, and chlorite near ore zones that have undergone regional metamorphism in the presence of fluids with a high sulfur content (Fullagar et al., 1967; Nesbitt, 1982).

Second, the Comus Formation basalts at Twin Creeks are unusually enriched in iron and potassium. The Comus basalts plot at compositions that are significantly higher in Fe_2O_3 relative to CaO and MgO than those of average basalts (Fig. 3D). Their composition is similar to iron-rich or ferrobasalts that have been observed in geologic settings, including modern midocean ridges (Clague and Bunch, 1976; Perfit and Fornari, 1983; Maury et al., 1985; Thy, 1985; Dixon et al., 1986), Tertiary rift zones (Leeman et al., 1976), Archean greenstone belts (Jackson and Smith, 1978), and lunar mares (Grove and Bence, 1979). Ferrobasalts commonly have elevated TiO_2 contents, which are also characteristic of the Comus Formation basalts (Bloomstein et al., 1991). Although alteration of these basalts has changed their composition, it is unlikely that this could account for their iron-rich nature. Additional support for a primary origin for the iron in these magmas is provided by the abundant, large, remnant Fe- Ti oxide phenocrysts, which account for a significant fraction of their total iron content.

The Comus Formation basalts are also enriched in potassium throughout most of the Megapit area. Samples from the Main sill inside the ore zone average 2.7 percent K_2O and the three samples of TC-5 Main sill outside the ore zone average 2.6 percent K_2O, compared to K_2O values of less than 0.6 percent in most fresh basalts (Irvine and Baragar, 1971; Gill, 1981; McBirney, 1983). Enrichment in potassium is more

widespread than gold mineralization and is not related to it, as indicated by the amount of potassium in Main sill samples from hole TC-5. As noted above, remobilization of potassium from igneous rocks in the ore zone probably accounts for the adularia associated with some gold mineralization at Twin Creeks. The potassium in these rocks is present as K feldspar, some of which replaces earlier plagioclase and some of which forms small crystals of uncertain origin in the groundmass. Potassium is not restricted to the Main sill, and high potassium values are typical of most basalts in the Twin Creeks area regardless of their degree of sericite-illite alteration. Sedimentary rocks are also enriched in potassium, as indicated by their abundant sericite and illite, although it is not clear whether the potassium was an original constituent of the sediments or was remobilized from the volcanic rocks.

Whether potassium in the igneous rocks is of magmatic or alteration origin is also unclear. Shoshonites and other potassic, mafic rocks can be associated with gold mineralization (Jensen and Barton, 2000; Mueller and Groves, 2000) and alkalic basalts have been reported from the Roberts Mountains allochthon (Poole et al., 1992). In a study of the Comus Formation in the Getchell area, Ten Brink (2002) recognized intermediate to ultramafic rocks with chemical signatures characteristic of a wide range of tectonic environments, some of which were alkalic. The Osgood stock or related intrusions probably formed the coarse-grained muscovite-calcite alteration beneath the northern (Chimney Creek) part of the Twin Creeks deposit (Hall et al., 2000), and might have caused potassic alteration at Twin Creeks. Biotite similar to that found in porphyry copper systems is seen in altered rocks around hole CTW-150, but no other evidence supports the presence of this type of mineralization. Seawater interaction is unlikely as well; the potassium contents of seawater are low and large amounts of potassium are not fixed in basalt during low-temperature metamorphism (Mottl and Seyfried, 1980). Potassic spilites reported from other areas appear to have formed on alkali-rich basalt in which potassium is redistributed at the sample and outcrop scale rather than over large regions (Narebski et al., 1986; Mengel et al., 1987; Lago et al., 1995; Moore, 1995; Ping, 1999). A comprehensive study of the petrogenesis of Comus Formation igneous rocks and the age of its potassium metasomatism is needed to resolve these questions.

Conclusions and Implications for Sulfidation as a Mechanism for Deposition of Gold in Carlin-type Gold Deposits

This study suggests that carbonate minerals in sedimentary rocks that were sulfidized to form the Twin Creeks gold deposit were enriched in iron which was released from interbedded igneous rocks during postdiagenetic hydrothermal alteration. This process differs from diagenetic processes normally responsible for the formation of iron-bearing carbonates in sedimentary rocks. Pyrite is the most common iron-bearing mineral that forms during diagenesis of sediments, usually as seawater sulfate is reduced to react with iron in the sediment. Formation of pyrite can be limited, however, in sulfate-poor diagenetic environments, leading to an increase of iron in diagenetic carbonate minerals (Canfield, 1989, 1991; Raiswell and Canfield, 1998). At Twin Creeks, additional iron appears to have been added by later hydrothermal alteration.

Recognition that rocks containing iron-rich carbonate can form by nondiagenetic processes is important to models for formation of any type of deposit in which gold is precipitated from solution by sulfidation of carbonate- bearing wall rock. In the Comus Formation, the most likely alternative processes involve interaction between iron- bearing igneous rocks and adjacent or interlayered sedimentary rocks. Iron-rich igneous rocks intrude sedimentary host rocks and have been thrust over receptive sedimentary rocks. In both cases, iron appears to have been liberated by alteration of iron-bearing phases, whether primary or secondary in the igneous rocks. The Comus basalts appear to have been significantly richer in iron than normal basalts and, as such, would have contributed much more iron to the interlayered sedimentary rocks. The potassic composition of the basalts does not appear to have been as important to iron exchange but might have been important because some rocks of this type show primary iron enrichment. Lack of information on the distribution of ferrobasalts in northern Nevada limits the degree to which these insights can be applied to the selection of areas for possible exploration in this area. Attention, however, should obviously be directed toward areas of alkalic basalt that are interlayered with carbonate-bearing shale.

Acknowledgments

This study was supported by National Science Foundation grant EAR 9804963 to S.E.K. Additional support was provided by the Santa Fe Pacific Gold Corporation, now a subsidiary of the Newmont Mining Company. During our work at Twin Creeks, we benefited from discussions and field sessions with many Santa Fe and Newmont geologists, particularly Bob Felder, Ron Parrat, Dean Peltonen, Charles Tapper, and Ron Thoreson. At the University of Michigan, we benefited from discussions with Jeff Alt, Eric Essene, and Grigore Simon. Earlier versions of this manuscript benefited from careful reviews by Greg Arehart, Al Hofstra, David John, and John Muntean.

REFERENCES

Alt, J.C., 1999, Very low-grade hydrothermal metamorphism of basic igneous rocks, *in* Frey, M., and Robinson, D., eds., Low-grade metamorphism: London, Blackwell Science, p. 169–201.

Alt, J.C., Laverne, C., and Muelenbachs, K., 1985, Alteration of the upper oceanic crust: Mineralogy and processes in DSDP hole 504B, leg 83: Deep Sea Drilling Project Initial Reports, v. 83, p. 217–247.

Alt, J.C., Teagle, D.A.H., Brewer, T., Shanks, W.C., III, and Halliday, A., 1998, Alteration and mineralization of an oceanic forearc and the ophiolite-ocean crust analogy: Journal of Geophysical Research, v. 103, p. B12,365–12,380.

Bloomstein, E.I., Massengill, G., Parrat, R.L., and Peltonen, D.R., 1991, Discovery, geology and mineralization of the Rabbit Creek gold deposit, Humboldt Country, Nevada, *in* Lisle, G.L., Schafer, R.W., and Wilkinson, W.H., eds., Geology and ore deposits of the Great Basin: Reno, Geological Society of Nevada, Symposium proceedings, p. 821–843.

Bryndzia, T., and Scott, S.D., 1987, The composition of chlorite as a function of sulfur and oxygen fugacity: An experimental study: American Journal of Science, v. 287, p. 50–76.

Cail, T.L., and Cline, J.S., 2001, Alteration associated with gold deposition at the Getchell Carlin-type gold deposit, north-central Nevada: Economic Geology, v. 96, p. 1343–1361.

Canfield, D.E., 1989, Reactive iron in marine sediments: Geochimica et Cosmochimica Acta, v. 53, p. 2483–2490.

——1991, Sulfate reduction in deep-sea marine sediments: American Journal of Science, v. 291, p. 177–188.

Clague, D.A., and Bunch, T.E., 1976, Formation of ferrobasalt at East Pacific midocean spreading centers: Journal of Geophysical Research, v. 81, p. B4247–4256.

Cline, J.S., 1999, Timing of gold and arsenic sulfide mineral deposition at the Getchell Carlin-type gold deposit, north-central Nevada: ECONOMIC GEOLOGY, v. 96, p. 75–89.
Crafford, E.J., 2000, Overview of regional geology and tectonic setting of the Osgood Mountains regions, Humboldt County, Nevada: Society of Economic Geologists Guidebook Series, v. 32, p. 225–234.
Dixon, J.E., Clague, D.A., and Eissen, J.-P., 1986, Gabbroic xenoliths and host ferrobasalt from the southern Juan de Fuca Ridge: Journal of Geophysical Research, v. 91, p. B3795–3820.
Ferguson, H.G., Roberts, R.J., and Muller, S.W., 1952, Geology of the Golconda quadrangle, Nevada: U.S. Geological Survey Bulletin 723, 163 p.
Fullagar, P.D., Brown, H.S., and Hagner, A.F., 1967, Geochemistry of wall-rock alteration and the role of sulfurization in the formation of the Ore Knob sulfide deposit: ECONOMIC GEOLOGY, v. 62, p. 798–825.
Gill, J.B., 1981, Orogenic andesites and plate tectonics: New York, Springer Verlag, 284 p.
Groff, J.A., Heizler, M.T., McIntosh, W.C., and Norman, D.I., 1997, $^{40}Ar/^{39}Ar$ dating and mineral paragenesis for Carlin-type gold deposits along the Getchell trend, Nevada: Evidence for Cretaceous and Tertiary gold mineralization: ECONOMIC GEOLOGY, v. 92, p. 601–623.
Grove, T.L., and Bence, A.E., 1979, Crystallization kinetics in a multiply saturated basalt magma: An experimental study of Luna 24 ferrobasalt, *in* Merrill, R.B., Bogard, D.D., McKay, D.S., and Robertson, P.C., eds., Proceedings of the Lunar and Planetary Science Conference: Houston, Lunar Science Institute, v. 1, p. 439–478.
Haggerty, S.E., 1976, Opaque mineral oxides in terrestrial igneous rocks, *in* Rumble, D., ed., Oxide minerals: Mineralogical Society of America Short Course Notes, v. 3, 200 p.
Hall, A., 1990, Geochemistry of spilites from south-west England; a statistical approach: Mineralogy and Petrology, v. 41, p. 185–197.
Hall, C.M., Kesler, S.E., Simon, G., and Fortuna, J., 2000, Overlapping Cretaceous and Eocene alteration, Twin Creeks Carlin-type deposit, Nevada: ECONOMIC GEOLOGY, v. 95, p. 1739–1752.
Hofstra, A.H., 1994, Geology and genesis of the Carlin-type gold deposits in Jerritt Canyon district, Nevada: Unpublished Ph.D. dissertation, Boulder, University of Colorado, 791 p.
Hofstra, A.H., and Cline, J.S., 2000, Characteristics and models for Carlin-type gold deposits: Reviews in Economic Geology, v. 13, p. 163–220.
Hofstra, A.H., Leventhal, J.S., Northrop, H.R., Landis, G.P., Rye, R.O., Birak, D.J., and Dahl, A.R., 1991, Genesis of sediment-hosted disseminated-gold deposits by fluid mixing and sulfidation: Chemical-reaction-path modeling of ore depositional processes documented in the Jerritt Canyon district, Nevada: Geology, v. 19, p. 36–40.
Hotz, P.E., and Wilden, R., 1964, Geology and mineral deposits of the Osgood Mountains quadrangle, Humboldt County, Nevada: U.S. Geological Survey Professional Paper 431, 128 p.
Irvine, T.N. and Baragar, W.R.A., 1971, A guide to the chemical classification of the common volcanic rocks: Canadian Journal of Earth Sciences, v. 8, p. 523–546.
Jackson, M.C. and Smith, I.E.M., 1978, Major and REE chemistry of Archean ferrobasalts, Abitibi greenstone belt, Ontario [abs.]: Geological Society of America Abstracts with Programs, v. 10, p. 428.
Kuehn, C.A. and Rose, A.W., 1992, Geology and geochemistry of wall-rock alteration at the Carlin gold deposit, Nevada: ECONOMIC GEOLOGY, v. 87, p. 1697–1721.
——1995, Carlin gold deposits, Nevada: Origin in a deep zone of mixing between normally pressured and overpressured fluids: ECONOMIC GEOLOGY, v. 90, p. 17–36.
Jensen , E.P., and Barton, M.D., 2000, Gold deposits related to alkaline magmatism: Reviews in Economic Geology, v. 13, p. 279–314.
Lago, M., Dumitrescu, R., Arranz, E., Bastida, J., Pocovi, A., Lopez Buendia, A., Martinez Gonzalez, R.M., Gil-Imaz, A., Lapuente, M.P., Vaquer, R., and Auque, L., 1995, Distinctive characters of three magmatisms, Triassic-Liassic, in the Iberian chain (Spain) [abs.]: Terra Abstracts, v. 7, Abstract Supplement 1, p. 180.
Leeman, W.P., Vitaliano, C.J.. and Prinz, M., 1976, Evolved lavas from the Snake River plain; Craters of the Moon National Monument, Idaho: Contributions to Mineralogy and Petrology, v. 56, p. 35–60.
Maury, R.C., Bougault, H., Coutelle, A., Guennoc, P., Joron, J.L., and Pautot, G., 1985, Presence de ferrobasalte tholeitique dans la fosse Jean-Charcot (26 degrees 15'N, 35 degrees 22'E); signification dans le contexte geodynamique de la Mer Rouge: Comptes Rendus de l'Academie des Sciences, Ser. 2, Sciences de la Terre, v. 300, p. 811–816.
McBirney, A.R., 1983, Igneous petrology: San Francisco, Freeman, Cooper, 462 p.
Mengel, K., Borsuk, A.M., Gurbanov, A.G., Wedepohl, K.H., Baumann, A., and Hoefs, J., 1987, Origin of spilitic rocks from the southern slope of the Greater Caucasus: Lithos, v. 20, no. 2, p. 115–133.
Moore, P.R., 1995, A Jurassic chert-limestone-spilite association near Eketahuna, North Island, New Zealand: Journal of the Royal Society of New Zealand, v. 25, no.2, p. 99–114.
Mottl, M.J., 1983, Hydrothermal processes at seafloor spreading centers: Application of basalt-seawater experimental results, *in* Rona, P.A., Bostrom, K., Laubier, L. and Smith, K.L., eds., Hydrothermal processes at seafloor spreading centers: New York, Plenum Press, p. 199–224.
Mottl, M.J. and Seyfried, W.E., 1980, Sub-seafloor hydrothermal systems; rock-vs. seawater-dominated, *in* Rona, P.A. and Lowell, R.P., eds., Seafloor spreading center hydrothermal systems: Stroudsburg, Pennsylvania, Dowden, Hutchinson and Ross, p. 88–82.
Mueller, D. and Groves, D.I., 2000, Potassic igneous rocks and associated gold-copper mineralization: Springer-Verlag, 252 p.
Narebski, W., Dostal, J., and Dupuy, C. 1986, Geochemical characteristics of lower Paleozoic spilite-keratophyre series in the Western Sudetes (Poland); petrogenic and tectonic implications: Neues Jahrbuch für Mineralogie Abhandlung, v.155, p. 243–258.
Nesbitt, B.E., 1982, Metamorphic sulfide-silicate equilibria in the massive sulfide deposits at Ducktown, Tennessee: ECONOMIC GEOLOGY, v. 77, p. 364–378.
Osterberg, M.W., 1990, Geology and geochemistry of the Chimney Creek gold deposit, Humboldt County, Nevada: Unpublished Ph.D. thesis, Tucson, University of Arizona, 173 p.
Osterberg, M.W. and Guilbert, J.M., 1991, Geology, wall-rock alteration, and new exploration techniques at the Chimney Creek sediment-hosted gold deposit, Humboldt County, Nevada, *in* Raines, G.L., Lisle, R.E., Schafer, R.W., and Wilkinson, W.H., eds., Geological Society of Nevada, Geology and Ore Deposits of the American Cordillera Symposium: Reno-Sparks, Nevada, April 1990, Proceedings, p. 805–819.
Perfit, M.R. and Fornari, D.J., 1983, Geochemical studies of abyssal lavas recovered by DSRV Alvin from eastern Galapagos rift, Inca transform, and Ecuador rift 2. Phase chemistry and crystallization history: Journal of Geophysical Research, v. 88, p. B10,530–10,550.
Ping, R., 1999, Discovery of potassic spilite (or poenite) in Langshan Group of Tanyaokou district, Inner Mongolia, China: Chinese Science Bulletin, v. 44, p. 563–567.
Poole, F.G., Stewart, J.H., Parmer, A.R., Sandberg, C.A., Madrid, R.J., Ross, R.J., Jr., Hintze, L.F., Miller, M.M. and Wrucke,C.T., 1992, Latest Precambrian to latest Devonian time; Development of a continental margin *in* Burchfiel, B.C., Lipman, P.W., and Zoback, M.L., eds., The Cordilleran orogen: Conterminous U.S.: Boulder, Colorado, Geological Society of America, The Geology of North America, v. G-3, p. 9–56.
Popp, R.K., 1976, Wallrock alteration associated with massive sulfide deposits, Ducktown, Tennessee: Carnegie Institute Washington Yearbook, 76-77, p. 603–607.
Raiswell, R. and Canfield, D.E., 1898, Sources of iron for pyrite formation in marine sediments: American Journal of Science, v. 298, p. 219–245.
Rumble, D., 1976, Oxide minerals in metamorphic rocks. Oxide minerals: Mineralogical Society of America Short Course Notes, v. 3, 24 p.
Seyfried, W.E., 1987, Experimental and theoretical constraints on hydrothermal alteration processes at mid-ocean ridges: Annual Reviews Earth and Planetary Science Letters, v. 15, p. 317–335.
Shau, Y.-H. and Peacor, D.R., 1992, Phyllosilicates in hydrothermally altered basalts from DSDP hole 504B, leg 83—a TEM and AEM study: Contributions to Mineralogy and Petrology, v. 12, p. 119–133.
Shau, Y.-H., Peacor, D.R. and Essene, E.J., 1990, Corrensite and mixed-layer chlorite/ corrensite in metabasalt from northern Taiwan; TEM/AEM, EMPA, XRD, and optical studies: Contributions to Mineralogy and Petrology, v. 105, p. 123–142.
Silberling, N.J. and Roberts, R.J., 1962, Pre-Tertiary stratigraphy and structure of northwest Nevada: Geological Society of America Special Paper 72, 58 p.
Silberman, M.L., Berger, B.R. and Koski, R.A., 1974, K-Ar age relations of granodiorite emplacement and W and Au mineralization near the Getchell mine, Humboldt County, Nevada: ECONOMIC GEOLOGY, v. 69, p. 646–656.
Simon, G., Kesler, S.E., and Chryssoulis, 1999, Geochemistry and textures of gold-bearing arsenian pyrite, Twin Creeks, Nevada: Implications for depositions of gold in Carlin-type deposits: ECONOMIC GEOLOGY v. 94, p. 405–422.

Stenger, D. P., Kesler, S.E., Peltonen, D.R. and Tapper, C.J., 1998, Deposition of gold in Carlin-type gold deposits: The role or sulfidation and decarbonatization at Twin Creeks, Nevada: ECONOMIC GEOLOGY, v. 93, p. 201–216.

Ten Brink, R., 2002, Geochemical characterization, elemental gain-loss, and geochronology of igneous rocks along the Getchell trend, northern Nevada: Geological Society of America Annual Meeting Paper no. 121-2 <http://gsa.confex.com/gsa/2002AM/finalprogram/abstract_40113.htm>.

Thoreson, R.F., Jones, J.E., Breit, F.J., Jr., Doyle-Kunkle, M.A. and Clarke, L.J., 2000, The geology and gold mineralization of the Twin Creeks gold deposits, Humboldt County, Nevada: Society of Economic Geologists Guidebook Series, v. 32, p. 175–187.

Thy, P., 1985, Chemical diversity in basaltic glasses and the origin of ferrobasalts at oceanic spreading centers [abs.]: EOS Transactions, American Geophysical Union, v. 66, p. 1108.

Tso, J., Gilbert, C. and Craig, J.R., 1979, Sulfidation of synthetic biotite: Experiment, theory and application: American Mineralogist, v. 64, p. 304–316.